Plug-and-play Voltage Stabilization in Inverter-interfaced Microgrids via a Robust Control Strategy

Mahdieh S. Sadabadi, Qobad Shafiee, and Alireza Karimi

***Abstract*—This paper proposes a decentralized control strategy for the voltage regulation of islanded inverter-interfaced microgrids. We show that an inverter-interfaced microgrid under plug-and-play (PnP) functionality of distributed generations (DGs) can be cast as a linear time-invariant (LTI) system subject to polytopic-type uncertainty. Then, by virtue of this novel description and use of the results from theory of robust control, the microgrid control system guarantees stability and a desired performance even in the case of PnP operation of DGs. The robust controller is a solution of a convex optimization problem. The main properties of the proposed controller are that 1) it is fully decentralized and local controllers of DGs use only local measurements, 2) the controller guarantees the stability of the overall system, 3) the controller allows plug-and-play functionality of DGs in microgrids, 4) the controller is robust against microgrid topology change. Various case studies, based on time-domain simulations in MATLAB/SimPowerSystems Toolbox, are carried out to evaluate the performance of the proposed control strategy in terms of voltage tracking, microgrid topology change, plug-and-play capability features, and load changes.**

***Index Terms*—Decentralized control, inverters, microgrids, plug-and-play capability, robust control, voltage control.**

I. Introduction

Reliable integration of distributed generations (DGs) into power systems can be achieved by means of microgrids which are small electrical networks heterogeneously composed of DGs, loads, and energy storage systems [1]. Renewable energy sources are normally interfaced to the microgrid through power electronic converters acting as voltage sources [2].

Microgrids normally operate in grid-connected mode where they are connected to the main grid at Point of Common Coupling (PCC). Under this connection scheme, the voltage and frequency of the microgrids are predominantly determined by the main grid while the microgrid control system accurately shares active and reactive power among DGs and controls the power exchange between the microgrid and the main grid [3]. Due to intentional (scheduled)/unintentional reasons, the microgrids can experience islanding conditions where they are disconnected from the main grid [4]. In this case, due to the power mismatch between the DGs and the loads, voltage and frequency of the loads deviate from their rated values and the islanded microgrid eventually becomes unstable. This operation mode of the microgrids is more challenging than the grid-connected mode because accurate load sharing mechanisms are required to balance the power mismatch [1]. Therefore, upon the islanding condition, a new microgrid control strategy must come into service in order to provide voltage and frequency stability as well as a proper power sharing among DGs [5].

In spite of the potential benefits that the use of DGs may bring, their increasing penetration challenges an appropriate control strategy to ensure stable and reliable operation of microgrids in both grid-connected and islanded modes and smooth transition between them [6]. The main challenges arise from basic differences existing between the physical characteristics of the conventional electrical generators and the inverter-interfaced microgrids [7]. Conventional power networks feature a large fraction of generation from traditional synchronous generators that present large rotational inertia and play a key role in maintaining frequency and voltage stability. Given current and future trends in the cost and regulation of distributed photovoltaic systems, the future power network will feature deep penetration of inverter-interfaced microgrids (see, e.g., the SunShot Initiative by the Department of Energy (DOE) in the USA[1]). While larger renewable penetration is desirable, current power-electronic inverters behave as low-inertia devices and are not designed to contribute to grid-wise stability.

One of the main problems associated with the control of microgrids is plug-and-play (PnP) functionality of DGs and microgrid topology change. DGs frequently join and leave the power generation system due to availability and intermittency of renewable energies, such as solar power and wind, an increase in energy demand, faults, maintenance, etc. Under PnP operation, different DGs are arbitrarily plugged-in or plugged-out from the microgrid; however, voltage and frequency of the local loads have to be stabilized without retuning the microgrid control system, in the absence of any communication link. Therefore, a decentralized control strategy is necessary to guarantee the stability of the microgrid system in the case of PnP functionality of DGs.

A control strategy ubiquitously used for the control of

This research work is financially supported by the Swiss National Science Foundation under Grant No. 200020-130528.

M. S. Sadabadi is with the Division of Automatic Control, Department of Electrical Engineering, Linköping University, Linköping, Sweden (e-mail: mahdieh.sadabadi@liu.se).

Q. Shafiee is with the Department of Electrical & Computer Engineering, University of Kurdistan, Sanandaj, Kurdistan, Iran (e-mail: q.shafiee@uok.ac.ir).

A. Karimi is with the Automatic Control Laboratory at Ecole Polytechnique Fédérale de Lausanne (EPFL), Lausanne, Switzerland (e-mail: alireza.karimi@epfl.ch).

[1] http://energy.gov/eere/sunshot/sunshot-initiative

microgrids is droop control which relies on the principle of power balance of a classical synchronous generator in conventional power networks (see, e.g., [2], [8]–[17]). In the power systems based on rotating generators, frequency (rotor speed) is dependent on active power balance, i.e. the frequency is dropped when the injected active power increases [18]. The idea of the so-called "droop" controllers has been developed by Chandorkar *et al* [19]. From a control point of view, droop control is a decentralized proportional controller maintaining the voltage and frequency stability of the microgrids [7]. One of the main advantage of droop-based control is the elimination of the communication links among droop controllers enabling the plug-and-play (PnP) operation in the microgrids. Moreover, primary droop control strategy provides proportional power sharing among DGs. Nonetheless, droop controllers with only a single tunable parameter drastically limit the achievable performance, especially during transients. Moreover, this control approach suffers from several drawbacks including load-dependent frequency/voltage deviation, coupled dynamics between active and reactive power, and poor performance in the case of resistive-inductive line conditions (mixed lines) and in the presence of conductances [20], [21].

In addition to the droop-based control strategies, non-droop-based approaches for voltage and frequency control of the islanded microgrids have also been developed, e.g. [20], [22]–[33]. Various voltage controller design methods such as robust servomechanism controllers [20], [23], [26], full-order H_∞ controllers [24], robust two-degree-of-freedom control strategy [28], multivariable voltage control scheme based on loop-shaping approaches [27], decentralized state feedbacks [29], and robust fixed-order decentralized H_∞ control approach [30] have been proposed. The proposed methods regulate the voltage of a single-DG [22]–[24], [27], [28] and/or a multi-DG microgrid [20], [26], [29]–[34]. In these methods, the frequency of each DG is controlled through an internal oscillator in an open-loop manner with $\omega_0 = 2\pi f_0$, where f_0 is the nominal system frequency. All oscillators are synchronized by a common time reference signal according to a global positioning system (GPS) [20]. In non-droop-based methods, power sharing is achieved via a power management system (PMS) which centrally solves an optimal power flow problem and broadcasts respective setpoints to DGs [20], [35]. In these approaches, the accuracy of the proportional load sharing is determined by how often the optimal power flow problem is solved and is not guaranteed during a load change.

Under PnP functionality of DGs and microgrid topology change, non-droop-based controllers, which rely on the system model, need to retune all their local controllers in order to guarantee the stability of the new system. Recently, a decentralized control strategy has been developed in [29], [34] which is based on a Quasi-Stationary Line (QSL) approximated model of microgrids [36] and the idea of neutral interactions [37]. According to this control technique, when a DG is plugged in and/or plugged out, the other DGs which are physically connected to it have to retune their local controllers. Although extensive research has been carried out on the development of droop and non-droop-based control of micorgrids, the problem of plug-and-play voltage stabilization in the inverter-interfaced microgrids is still open and can benefit from further research.

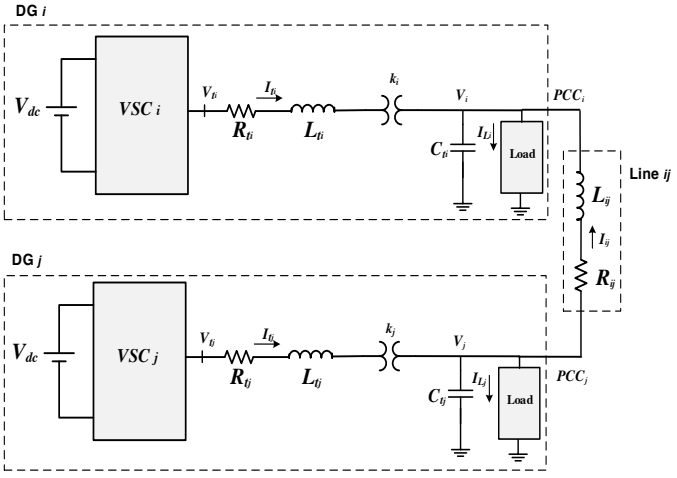

Fig. 1. Electrical scheme of two DGs connected via line ij.

In this paper, a solution for the problem of PnP functionality of DGs is presented. We show that an inverter-interfaced microgrid consisting of multi DGs under plug-and-play functionality can be cast as a linear time-invariant (LTI) system with polytopic uncertainty. By virtue of this novel description and use of the results from theory of robust control, the stability of the microgrid system under PnP operation of DGs is preserved. Therefore, opposed to most non-droop-based control methods, e.g. [20], [26], [29], [30], [34], the present approach does not require to retune the local controllers in the case of PnP operation of DGs and topology change. Moreover, unlike the droop control strategy, the proposed approach guarantees the stability of the microgrid system under PnP functionality of DGs. To verify the performance of the proposed control approach, it is applied to a microgrid system composed of 11 DGs. The performance of the controller is verified using simulation case studies carried out in MATLAB/SimPowerSystems. The obtained results confirm the effectiveness of the proposed controller against PnP operation of DGs and microgrid topology change.

The organization of the paper is as follows: The mathematical model of the microgrid is presented in Section II. Sections III is devoted to the islanded microgrid control system. A solution for the problem of plug-and-play operation of DGs in the microgrids is given in Section IV. Section V is devoted to simulation results. Section VI concludes the paper.

Throughout the paper, matrices I and 0 are the identity matrix and the zero matrix of appropriate dimensions, respectively. The symbols T and $\star$ denote the matrix transpose and a symmetric block, respectively. Signals X_d and X_q are the d and q components of the three-phase signal X, respectively. For symmetric matrices, $P > 0$ ($P < 0$) indicates the positive-definiteness (the negative-definiteness).

II. Islanded Microgrid Model

Consider an islanded microgrid with general structure consisting of N DGs. Each DG is modeled as a DC voltage source, a voltage-source converter (VSC), a series RL filter, a step-up transformer with transformation ratio k_i, a shunt capacitor, and a local load whose topology and parameters are unknown.

It is assumed that DG i is connected to a set of $N_i \subset \{1,\dots,N\}$ DGs. The schematic diagram of a microgrid system of two DGs, DG i and DG j, connected through a transmission line ij is shown in Fig. 1. In this figure, V_i, I_{t_i}, I_{L_i}, V_{t_i}, and I_{ij} are the load voltage at PCC i, the filter current, the load current, the VSC terminal voltage, and the transmission line current, respectively. Under balanced conditions, the islanded system is described by the following dynamical equations in dq-frame:

$$\text{DG } i \begin{cases} \frac{dV_{i,dq}}{dt} + j\omega_0 V_{i,dq} = \frac{k_i}{C_{ti}} I_{ti,dq} - \frac{1}{C_{ti}} I_{L_i,dq} + \frac{1}{C_{ti}} I_{ij,dq} \\ \frac{dI_{ti,dq}}{dt} + j\omega_0 I_{ti,dq} = -\frac{k_i}{L_{ti}} V_{i,dq} - \frac{R_{ti}}{L_{ti}} I_{ti,dq} + \frac{1}{L_{ti}} V_{ti,dq} \end{cases} \tag{1}$$

$$\text{DG } j \begin{cases} \frac{dV_{j,dq}}{dt} + j\omega_0 V_{j,dq} = \frac{k_j}{C_{tj}} I_{tj,dq} - \frac{1}{C_{tj}} I_{L_j,dq} - \frac{1}{C_{tj}} I_{ij,dq} \\ \frac{dI_{tj,dq}}{dt} + j\omega_0 I_{tj,dq} = -\frac{k_j}{L_{tj}} V_{j,dq} - \frac{R_{tj}}{L_{tj}} I_{tj,dq} + \frac{1}{L_{tj}} V_{tj,dq} \end{cases} \tag{2}$$

$$\text{Line } ij: \quad \frac{dI_{ij,dq}}{dt} + j\omega_0 I_{ij,dq} = -\frac{R_{ij}}{L_{ij}} I_{ij,dq} + \frac{1}{L_{ij}} V_{j,dq} - \frac{1}{L_{ij}} V_{i,dq} \tag{3}$$

where $(V_{i,dq}, V_{j,dq})$, $(I_{ti,dq}, I_{tj,dq})$, $(I_{L_i,dq}, I_{L_j,dq})$, $(V_{ti,dq}, V_{tj,dq})$, and $I_{ij,dq}$ respectively are the dq components of the load voltages at PCCs, the current filters, the load currents, the VSC terminal voltages, and the transmission line current. It should be noted that in this study the dynamics of the renewable energy sources are not considered and they are just modeled by an ideal voltage source.

Under the assumption of Quasi-Stationary Line (QSL) [36], i.e. $\frac{dI_{ij,dq}}{dt} = 0$, the line dynamics in (3) is written as follows:

$$I_{ij,dq} = \frac{V_{j,dq} - V_{i,dq}}{R_{ij} + j\omega_0 L_{ij}} \tag{4}$$

By replacing $I_{ij,dq}$ in (1) and (2) with (4), the islanded microgrid system is described in the following state space framework:

$$\begin{aligned} \dot{x}_{g_i} &= A_{g_{ii}} x_{g_i} + \sum_{j \in N_i} A_{g_{ij}} x_{g_j} + B_{g_i} u_i + B_{w_i} w_i \\ y_i &= C_{g_i} x_{g_i}; \quad i = 1,\dots,N \end{aligned} \tag{5}$$

where $x_{g_i} = \begin{bmatrix} V_{i,d} & V_{i,q} & I_{t_i,d} & I_{t_i,q} \end{bmatrix}^T$ is the state, $u_i = \begin{bmatrix} V_{t_i,d} & V_{t_i,q} \end{bmatrix}^T$ is the input, $w_i = \begin{bmatrix} I_{L_i,d} & I_{L_i,q} \end{bmatrix}^T$ is the exogenous input, and $y_i = \begin{bmatrix} V_{i,d} & V_{i,q} \end{bmatrix}^T$ is the output of DG i. The state space matrices are given as follows [29]:

$$\begin{aligned} A_{g_{ii}} &= \begin{bmatrix} -\frac{1}{C_{t_i}} \sum_{j \in N_i} \frac{R_{ij}}{Z_{ij}^2} & \omega_0 - \frac{1}{C_{t_i}} \sum_{j \in N_i} \frac{X_{ij}}{Z_{ij}^2} & \frac{k_i}{C_{t_i}} & 0 \\ -\omega_0 + \frac{1}{C_{t_i}} \sum_{j \in N_i} \frac{X_{ij}}{Z_{ij}^2} & -\frac{1}{C_{t_i}} \sum_{j \in N_i} \frac{R_{ij}}{Z_{ij}^2} & 0 & \frac{k_i}{C_{t_i}} \\ -\frac{k_i}{L_{t_i}} & 0 & -\frac{R_{t_i}}{L_{t_i}} & \omega_0 \\ 0 & -\frac{k_i}{L_{t_i}} & -\omega_0 & -\frac{R_{t_i}}{L_{t_i}} \end{bmatrix} \\ A_{g_{ij}} &= \frac{1}{C_{t_i}} \begin{bmatrix} \frac{R_{ij}}{Z_{ij}^2} & \frac{X_{ij}}{Z_{ij}^2} & 0 & 0 \\ -\frac{X_{ij}}{Z_{ij}^2} & \frac{R_{ij}}{Z_{ij}^2} & 0 & 0 \\ 0 & 0 & 0 & 0 \\ 0 & 0 & 0 & 0 \end{bmatrix}, \quad B_{g_i} = \begin{bmatrix} 0 & 0 \\ 0 & 0 \\ \frac{1}{L_{t_i}} & 0 \\ 0 & \frac{1}{L_{t_i}} \end{bmatrix} \\ B_{w_i} &= \begin{bmatrix} -\frac{1}{C_{t_i}} & 0 \\ 0 & -\frac{1}{C_{t_i}} \\ 0 & 0 \\ 0 & 0 \end{bmatrix}, \quad C_{g_i} = \begin{bmatrix} 1 & 0 & 0 & 0 \\ 0 & 1 & 0 & 0 \end{bmatrix} \end{aligned} \tag{6}$$

where $\omega_0 = 2\pi f_0$ (f_0 is the nominal frequency of the microgrid), $X_{ij} = \omega_0 L_{ij}$, and $Z_{ij}^2 = R_{ij}^2 + \omega_0^2 L_{ij}^2$.

A. QSL-based Model of Islanded Microgrids with N DGs

In a similar way, the overall model of the islanded microgrid system of N DGs can be described in the state space framework as follows:

$$\begin{aligned} \begin{bmatrix} \dot{x}_{g_1} \\ \dot{x}_{g_2} \\ \vdots \\ \dot{x}_{g_N} \end{bmatrix} &= \begin{bmatrix} A_{g_{11}} & A_{g_{12}} & \cdots & A_{g_{1N}} \\ A_{g_{21}} & A_{g_{22}} & \cdots & A_{g_{2N}} \\ \vdots & \vdots & \ddots & \vdots \\ A_{g_{N1}} & A_{g_{N2}} & \cdots & A_{g_{NN}} \end{bmatrix} \begin{bmatrix} x_{g_1} \\ x_{g_2} \\ \vdots \\ x_{g_N} \end{bmatrix} \\ &+ \begin{bmatrix} B_{g_1} & 0 & \cdots & 0 \\ 0 & B_{g_2} & \cdots & 0 \\ \vdots & \vdots & \ddots & \vdots \\ 0 & 0 & \cdots & B_{g_N} \end{bmatrix} \begin{bmatrix} u_1 \\ u_2 \\ \vdots \\ u_N \end{bmatrix} \\ &+ \begin{bmatrix} B_{w_1} & 0 & \cdots & 0 \\ 0 & B_{w_2} & \cdots & 0 \\ \vdots & \vdots & \ddots & \vdots \\ 0 & 0 & \cdots & B_{w_N} \end{bmatrix} \begin{bmatrix} w_1 \\ w_2 \\ \vdots \\ w_N \end{bmatrix} \\ \begin{bmatrix} y_1 \\ y_2 \\ \vdots \\ y_N \end{bmatrix} &= \begin{bmatrix} C_{g_1} & 0 & \cdots & 0 \\ 0 & C_{g_2} & \cdots & 0 \\ \vdots & \vdots & \ddots & \vdots \\ 0 & 0 & \cdots & C_{g_N} \end{bmatrix} \begin{bmatrix} x_{g_1} \\ x_{g_2} \\ \vdots \\ x_{g_N} \end{bmatrix} \end{aligned} \tag{7}$$

where matrices $A_{g_{ii}}$, $A_{g_{ij}}$, B_{g_i}, B_{w_i}, and C_{g_i} (for $i, j = 1,2,\dots,N$) are defined in (6). Matrix $A_{g_{ij}} = 0$ if and only if there exists no connection between DGs i and j.

III. Islanded Microgrid Control System

Consider a schematic diagram of the microgrid control strategy composed of a power management system (PMS), local voltage controllers of DGs, and a frequency control scheme in Fig. 2.

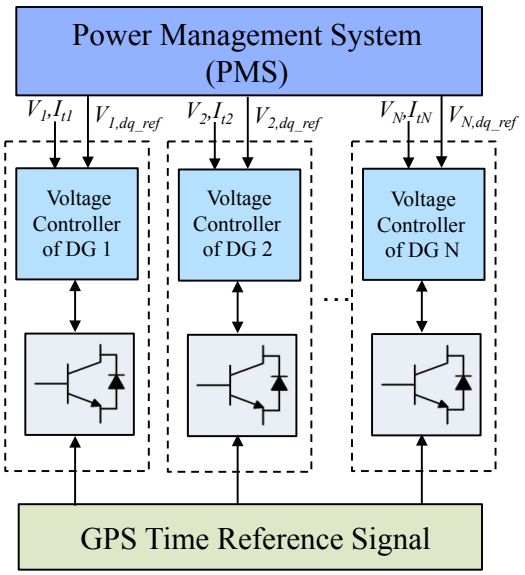

Fig. 2. General scheme of non-droop control approaches for islanded inverter-interfaced microgrids.

A. Power Management System

A power management strategy is required for reliable and efficient operation of a microgrid system with multiple DGs, particularly in the islanded mode of operation [38]. The main function of the power management system (PMS) is to maintain an optimal operating point for the microgrid. PMS assigns the active and reactive power set points for the DGs to (i) properly share the real and reactive power among the DGs based on either a cost function associated with each DG unit or a market signal [26], (ii) appropriately respond to the microgrid disturbances and major changes [39], (iii) balance the microgrid power, and (iv) provide the resynchronization of the microgrid system with the main grid, if required [39]. The set points are then transmitted to the local controllers of the DGs. The local controllers measure the voltage at their corresponding PCCs or the active/reactive output power of their own DG unit and then enable the voltage tracking according to the received reference set points [20].

B. Frequency Control

The frequency of the microgrid system is controlled in the open-loop. To this end, each DG unit includes an oscillator which generates $\theta(t) = \int_0^t \omega_0 d\tau$, where $\omega_0 = 2\pi f_0$ and f_0 is the nominal frequency of the microgrid. The phase-angle waveform $\theta(t)$ is employed for *dq*/*abc* (*abc*/*dq*) transformations. The DGs are then synchronized by a global synchronization signal that is communicated to the oscillators of DGs through the global positioning system (GPS) [26].

C. Voltage Control

The voltage set points are communicated from PMS to local controllers of the DGs and transformed to the *dq*-frame based on the phase-angle signal $\theta(t)$ generated by their internal oscillator. The main objective is to develop a decentralized voltage controller for the islanded operation of the inverter-interfaced microgrids given in (7). The focus of this paper is on the development of a voltage control strategy for autonomous microgrids. It can be applied to the microgrids with different types of configuration. The main emphasis is given to decentralized voltage control techniques which do not need any communication.

1) Design Requirements: A *dq*-based voltage controller for the islanded inverter-interfaced microgrid described in (7) is sought such that the following conditions are met:

- The controller has a fully decentralized structure.
- The closed-loop system is asymptotically stable.
- The closed-loop system asymptotically tracks all reference voltage signals y_{ref_i} with desired time-domain performance.

In the following, a decentralized voltage controller with integral action is developed in order to achieve all above mentioned conditions.

2) Decentralized Voltage Controllers: One of the control requirements is that DGs must track reference voltage signals, y_{ref_i}. To this end, each DG is augmented with an integrator whose dynamics are as follows:

$$\begin{aligned} \dot{v}_i &= y_{ref_i} - y_i \\ &= y_{ref_i} - C_{g_i} x_{g_i} \end{aligned} \tag{8}$$

Therefore, the augmented DG system is described by:

$$\begin{aligned} \dot{\hat{x}}_{g_i} &= \hat{A}_{g_{ii}} \hat{x}_{g_i} + \sum_{j \in N_i} \hat{A}_{g_{ij}} \hat{x}_{g_j} + \hat{B}_{g_i} u_i + \hat{B}_{w_i} \hat{w}_i \\ \hat{y}_i &= \hat{C}_{g_i} \hat{x}_{g_i} \end{aligned} \tag{9}$$

where $\hat{x}_{g_i} = \begin{bmatrix} x_{g_i}^T & v_i^T \end{bmatrix}^T$, $\hat{y}_i = \begin{bmatrix} y_i^T & v_i^T \end{bmatrix}^T$, $\hat{w}_i = \begin{bmatrix} w_i^T & y_{ref_i}^T \end{bmatrix}^T$, and

$$\begin{aligned} \hat{A}_{g_{ii}} &= \begin{bmatrix} A_{g_{ii}} & 0 \\ -C_{g_i} & 0 \end{bmatrix}, \quad \hat{A}_{g_{ij}} = \begin{bmatrix} A_{g_{ij}} & 0 \\ 0 & 0 \end{bmatrix} \\ \hat{B}_{g_i} &= \begin{bmatrix} B_{g_i} \\ 0 \end{bmatrix}, \quad \hat{B}_{w_i} = \begin{bmatrix} B_{w_i} & 0 \\ 0 & I \end{bmatrix} \\ \hat{C}_{g_i} &= \begin{bmatrix} C_{g_i} & 0 \\ 0 & I \end{bmatrix} \end{aligned} \tag{10}$$

The remains of this subsection belong to the design of decentralized voltage controllers K_i with the following control laws:

$$u_i(t) = K_i \hat{x}_{g_i}(t); \quad i = 1, 2, \ldots, N \tag{11}$$

The closed-loop dynamics of the i^{th} augmented subsystem with the local controller K_i are described as follows:

$$\begin{aligned} \dot{\hat{x}}_{g_i}(t) &= \big(\hat{A}_{g_{ii}} + \hat{B}_{g_i} K_i\big) \hat{x}_{g_i}(t) + \sum_{j \in N_i} \hat{A}_{g_{ij}} \hat{x}_{g_j}(t) + \hat{B}_{w_i} \hat{w}_i(t) \\ \hat{y}_i(t) &= \hat{C}_{g_i} \hat{x}_{g_i}(t) \end{aligned} \tag{12}$$

The overall closed-loop system is presented as follows:

$$\begin{aligned} \dot{\hat{x}}(t) &= \big(\hat{A} + \hat{B}K\big) \hat{x} + \hat{B}_w \hat{w}(t) \\ \hat{y}(t) &= \hat{C} \hat{x}(t) \end{aligned} \tag{13}$$

where $\hat{x} = \left[\hat{x}_{g_1}^T \dots \hat{x}_{g_N}^T\right]^T$, $\hat{w} = \left[\hat{w}_1^T \dots \hat{w}_N^T\right]^T$, $\hat{y} = \left[\hat{y}_1^T \dots \hat{y}_N^T\right]^T$, and

$$\begin{aligned}
\hat{A} &= \begin{bmatrix} \hat{A}_{g_{11}} & \hat{A}_{g_{12}} & \cdots & \hat{A}_{g_{1N}} \\ \hat{A}_{g_{21}} & \hat{A}_{g_{22}} & \cdots & \hat{A}_{g_{2N}} \\ \vdots & \vdots & \ddots & \vdots \\ \hat{A}_{g_{N1}} & \hat{A}_{g_{N2}} & \cdots & \hat{A}_{g_{NN}} \end{bmatrix} \\
\hat{B} &= \text{diag}\left(\hat{B}_{g_1}, \dots, \hat{B}_{g_N}\right) \\
\hat{B}_w &= \text{diag}\left(\hat{B}_{w_1}, \dots, \hat{B}_{w_N}\right) \\
\hat{C} &= \text{diag}\left(\hat{C}_{g_1}, \dots, \hat{C}_{g_N}\right) \\
K &= \text{diag}\left(K_1, \dots, K_N\right)
\end{aligned} \tag{14}$$

The state feedback controller is designed via the following theorem which is based on the use of slack variables [40].

Theorem 1. *There exists a state feedback controller K which stabilizes an open-loop system $G(s) = \left(\hat{A}, \hat{B}, \hat{C}, 0\right)$ if and only if there exist a symmetric matrix $P = P^T > 0$, slack matrices G, Y, and a positive scalar ε such that the following conditions hold:*

$$\begin{bmatrix} \hat{A}G + G^T\hat{A}^T + \hat{B}Y + Y^T\hat{B}^T & \star \\ P - G + \varepsilon\left(G^T\hat{A}^T + Y^T\hat{B}^T\right) & -\varepsilon\left(G + G^T\right) \end{bmatrix} < 0 \tag{15}$$

Moreover, the state feedback gain is presented as $K = YG^{-1}$.

For instance, assume that the coupling term $\sum_{j\in N_i}\hat{A}_{g_{ij}}\hat{x}_{g_j}$ can be neglected, then according to Theorem 1, the augmented subsystem of each DG $\left(\hat{A}_{g_{ii}}, \hat{B}_{g_i}, \hat{C}_{g_i}, 0\right)$ with the state feedback gain K_i is stable if and only if there exist Lyapunov matrices $P_i = P_i^T > 0$ and slack variables $G_i, Y_i, \varepsilon_i > 0$ such that

$$\begin{bmatrix} \hat{A}_{g_{ii}}G_i + G_i^T\hat{A}_{g_{ii}}^T + \hat{B}_{g_i}Y_i + Y_i^T\hat{B}_{g_i}^T & \star \\ P_i - G_i + \varepsilon_i\left(G_i^T\hat{A}_{g_{ii}}^T + Y_i^T\hat{B}_{g_i}^T\right) & -\varepsilon_i\left(G_i + G_i^T\right) \end{bmatrix} < 0 \tag{16}$$

for $i = 1, \dots, N$. The local state feedback controllers are presented as $K_i = Y_iG_i^{-1}$; $i = 1, \dots, N$. However, the interaction terms have significant effects on the stability of the closed-loop system and decentralized design of the local controllers cannot generally guarantee the stability of the whole system, i.e. $\hat{A}$. In the next subsection, we show that under some specific conditions, the stability conditions given in (16) lead to the overall closed-loop asymptotic stability.

3) Design Strategy based on Neutral Interactions: The main objective is to design the local controllers individually without considering the interaction terms such that the asymptotic stability of the closed-loop microgrid system is guaranteed. To this end, the idea of neutral interaction in [37] is used. The interaction terms are neutral with respect to the stability criterion in (15) if and only if the interaction matrix $\hat{A}_c = \hat{A} - \hat{A}_d$, where $\hat{A}_d = \text{diag}\left(\hat{A}_{g_{11}}, \dots, \hat{A}_{g_{NN}}\right)$, is factorized as follows:

$$\hat{A}_c = G^TS \tag{17}$$

where G is the slack matrix in (15) and S is a skew-symmetric matrix, i.e. $S^T = -S$.

Under the following conditions, the interaction terms in the augmented microgrid model described by (13)-(14) are neutral.

1) $C_{t_i} = C_s$ for $i = 1, \dots, N$.

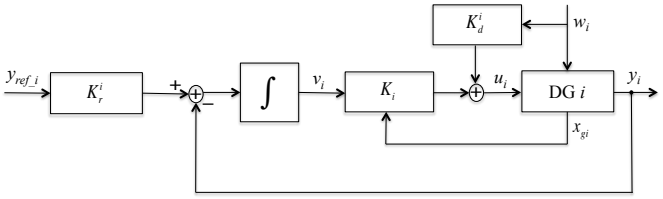

Fig. 3. Block diagram of 3DOF voltage controller.

2) The local state feedback controllers K_i satisfy the stability conditions given in (16) with the following fixed-structure slack matrices G_i:

$$G_i = \left[\begin{array}{c|c} \eta I_{2\times 2} & 0 \\ \hline 0 & G_{22_i} \end{array}\right]; \quad i = 1, \dots, N \tag{18}$$

where $\eta > 0$ is a common parameter among all G_i, $i = 1, \dots, N$ and matrices G_{22_i} are of appropriate dimensions.

3) $\frac{\eta R_{ij}}{C_sZ_{ij}^2} \approx 0$ for $i = 1, \dots, N$ and $j \in N_i$.

If the above mentioned conditions hold, the interaction terms $\hat{A}_{g_{ji}}G_j + G_j^T\hat{A}_{g_{ij}}^T \approx 0$ because

$$\hat{A}_{g_{ij}}G_j = \left[\begin{array}{c|c} \Phi_{ij} & 0 \\ \hline 0 & 0 \end{array}\right] \tag{19}$$

where $\Phi_{ij} = \begin{bmatrix} \frac{\eta R_{ij}}{C_sZ_{ij}^2} & \frac{\eta X_{ij}}{C_sZ_{ij}^2} \\ -\frac{\eta X_{ij}}{C_sZ_{ij}^2} & \frac{\eta R_{ij}}{C_sZ_{ij}^2} \end{bmatrix} \approx \begin{bmatrix} 0 & \frac{\eta X_{ij}}{C_sZ_{ij}^2} \\ -\frac{\eta X_{ij}}{C_sZ_{ij}^2} & 0 \end{bmatrix}$.

4) Pre-filter Design & Disturbance Rejection Strategy: Under the above-mentioned conditions, the decentralized state feedback controllers K_i designed by (16) guarantee the stability of the closed-loop microgrid system. However, to improve the performance of the system in terms of dynamics behaviour for voltage reference tracking and disturbance rejection, the local controllers are modified. The modification procedure is based on the use of a three-degree-of-freedom (3DOF) controller whose structure is shown in Fig. 3. The feedforward controller K_r^i is designed to improve reference tracking performance whereas K_d^i aims to attenuate the effects from the disturbance w_i on the output signals. The closed-loop system including the 3DOF controller in Fig. 3 is described as follows:

$$y_i = \left(T_i(s)K_r^i(s)\right)y_{ref_i} + \left(H_i(s)K_d^i(s) + H_i^d(s)\right)w_i \tag{20}$$

where

$$\begin{aligned}
T_i(s) &= \hat{C}_i\left(sI - \left(\hat{A}_{g_{ii}} + \hat{B}_{g_i}K_i\right)\right)^{-1}\begin{bmatrix} 0 \\ I \end{bmatrix} \\
H_i(s) &= \hat{C}_i\left(sI - \left(\hat{A}_{g_{ii}} + \hat{B}_{g_i}K_i\right)\right)^{-1}\hat{B}_{g_i} \\
H_i^d(s) &= \hat{C}_i\left(sI - \left(\hat{A}_{g_{ii}} + \hat{B}_{g_i}K_i\right)\right)^{-1}\hat{B}_{w_i}
\end{aligned} \tag{21}$$

To achieve desired time-domain performance specifications for reference tracking and minimize the effect of load changes on the voltages at PCCs, the controllers $K_r^i(s)$ and $K_d^i(s)$ are respectively designed by means of solving the following optimization problems:

$$\min_{K_r^i}\|T_i(s)K_r^i(s) - T_{d_i}(s)\|_\infty \tag{22}$$

$$\min_{K_d^i}\|H_i(s)K_d^i(s) + H_i^d(s)\|_\infty \tag{23}$$

where $T_{d_i}(s)$ is a desired reference tracking (reference model) designed according to the desired performance of DG unit i . To solve the above optimization problems, the MATLAB commands *hinfstruct*, *looptune*, and *systune* can be used.

IV. Plug-and-Play (PnP) Functionality

In this section, the problem of plug-in/-out operation in the islanded inverter-interfaced microgrids is considered. The objective is to preserve the stability of the microgrid system when several DGs are plugged in and/or plugged out.

A. Robustness to PnP Functionality of DGs

A new feature is added to the proposed decentralized control strategy which is robustness to PnP functionality. By virtue of the fact that the plug-in/-out of DG j to/from DG i affects only matrix $A_{g_{ii}}$, two cases for each DG are considered:

- Maximum possible connections of the DGs to DG i ($N_{i_{max}} \subset \{1,\dots,N\}$)
- Connection j with minimum values of $\frac{R_{ij}}{Z_{ij}^2}$ and $\frac{X_{ij}}{Z_{ij}^2}$ among the other connections.

$$\begin{aligned}\left(\frac{R}{Z^2}\right)_{min} &= \min_{j\in N_i} \frac{R_{ij}}{Z_{ij}^2} \\ \left(\frac{X}{Z^2}\right)_{min} &= \min_{j\in N_i} \frac{X_{ij}}{Z_{ij}^2}\end{aligned} \tag{24}$$

Corresponding matrix $A_{g_{ii}}$ for both cases are given as follows:

$$A_{g_{ii}}^1 = \begin{bmatrix} -\frac{1}{C_{t_i}}\sum_{j\in N_{i_{max}}}\frac{R_{ij}}{Z_{ij}^2} & \omega_0 - \frac{1}{C_{t_i}}\sum_{j\in N_{i_{max}}}\frac{X_{ij}}{Z_{ij}^2} & \frac{k_i}{C_{t_i}} & 0 \\ -\omega_0 + \frac{1}{C_{t_i}}\sum_{j\in N_{i_{max}}}\frac{X_{ij}}{Z_{ij}^2} & -\frac{1}{C_{t_i}}\sum_{j\in N_{i_{max}}}\frac{R_{ij}}{Z_{ij}^2} & 0 & \frac{k_i}{C_{t_i}} \\ -\frac{k_i}{L_{t_i}} & 0 & -\frac{R_{t_i}}{L_{t_i}} & \omega_0 \\ 0 & -\frac{k_i}{L_{t_i}} & -\omega_0 & -\frac{R_{t_i}}{L_{t_i}} \end{bmatrix}$$

$$A_{g_{ii}}^2 = \begin{bmatrix} -\frac{1}{C_{t_i}}\left(\frac{R}{Z^2}\right)_{min} & \omega_0 - \frac{1}{C_{t_i}}\left(\frac{X}{Z^2}\right)_{min} & \frac{k_i}{C_{t_i}} & 0 \\ -\omega_0 + \frac{1}{C_{t_i}}\left(\frac{X}{Z^2}\right)_{min} & -\frac{1}{C_{t_i}}\left(\frac{R}{Z^2}\right)_{min} & 0 & \frac{k_i}{C_{t_i}} \\ -\frac{k_i}{L_{t_i}} & 0 & -\frac{R_{t_i}}{L_{t_i}} & \omega_0 \\ 0 & -\frac{k_i}{L_{t_i}} & -\omega_0 & -\frac{R_{t_i}}{L_{t_i}} \end{bmatrix} \tag{25}$$

Therefore, any possible connection/disconnection of DGs to DG i belongs to the following polytopic uncertainty domain:

$$A_{g_{ii}}(\lambda) = \lambda A_{g_{ii}}^1 + (1-\lambda)A_{g_{ii}}^2 \tag{26}$$

where $0 \le \lambda \le 1$. As a result, matrices $\hat{A}_{g_{ii}}$ also have the polytopic uncertainty as follows:

$$\hat{A}_{g_{ii}}(\lambda) = \lambda \hat{A}_{g_{ii}}^1 + (1-\lambda)\hat{A}_{g_{ii}}^2 \tag{27}$$

where

$$\hat{A}_{g_{ii}}^1 = \begin{bmatrix} A_{g_{ii}}^1 & 0 \\ -C_{g_i} & 0 \end{bmatrix}, \quad \hat{A}_{g_{ii}}^2 = \begin{bmatrix} A_{g_{ii}}^2 & 0 \\ -C_{g_i} & 0 \end{bmatrix} \tag{28}$$

for $i = 1,\dots,N$.

Now, we aim to design a decentralized state feedback controller for the augmented polytopic system $\left(\hat{A}_{g_{ii}}(\lambda), \hat{B}_{g_i}, \hat{C}_{g_i}, 0\right)$ by means of the following theorem [40]:

Theorem 2. *If there exist symmetric matrices $P_i^j > 0$, slack matrices G_i, Y_i, and a given scalar $\varepsilon_i > 0$ such that the following set of LMIs holds*

$$\begin{bmatrix} \hat{A}_{g_{ii}}^j G_i + G_i^T(\hat{A}_{g_{ii}}^j)^T + \hat{B}_{g_i}Y_i + Y_i^T\hat{B}_{g_i}^T & \star \\ P_i^j - G_i + \varepsilon_i\left(\hat{A}_{g_{ii}}^j G_i + \hat{B}_{g_i}Y_i\right)^T & -\varepsilon_i\left(G_i + G_i^T\right) \end{bmatrix} < 0 \tag{29}$$

for $j = 1,2$. Then, the state feedback gain $K_i = Y_i G_i^{-1}$ stabilizes the system $\left(\hat{A}_{g_{ii}}(\lambda), \hat{B}_{g_i}, \hat{C}_{g_i}, 0\right)$ via a linearly parameter-dependent Lyapunov matrix $P_i(\lambda) = \lambda P_i^1 + (1-\lambda)P_i^2$, where $0 \le \lambda \le 1$.

Remark. In the case of microgrids with radial (parallel) configuration, three cases happen for the disconnection of DGs from DG i: 1) disconnection of DG $i-1$ and DG $i+1$, 2) disconnection of only DG $i-1$, and 3) disconnection of only DG $i+1$. Therefore, the connection/disconnection of DGs to DG i in a radial or parallel microgrid can be described by a multi-model uncertainty composed of four models where the set of DGs connected to DG i is 1) $N_i = \{\}$, 2) $N_i = \{i-1\}$, 3) $N_i = \{i+1\}$, and 4) $N_i = \{i-1, i+1\}$.

B. Algorithm I: "Decentralized Control of Islanded Inverter-interfaced Microgrids"

In this subsection, a systematic algorithm for the design of the local state feedback controllers K_i for the DG i described by (5)-(6) under plug-and-play functionality is given. The algorithm consists of the following steps:

Step 1: Build two vertices $A_{g_{ii}}^1$ and $A_{g_{ii}}^2$ given in (25) as well as augmented matrices $\hat{A}_{g_{ii}}^1$ and $\hat{A}_{g_{ii}}^2$ in (28), for $i = 1,\dots,N$.

Step 2: Impose the structural constraints given in (18) on the slack matrix G_i in (29).

Step 3: Fix the scalar parameter $\varepsilon_i > 0$ in (29) and solve the following convex optimization problem to obtain the state feedback controllers K_i:

$$\begin{aligned} \min_{Y_i, P_i^j, \eta, G_{22_i}} \quad & \eta \\ \text{subject to} \quad & \begin{bmatrix} \hat{A}_{g_{ii}}^j G_i + G_i^T(\hat{A}_{g_{ii}}^j)^T + \hat{B}_{g_i}Y_i + Y_i^T\hat{B}_{g_i}^T & \star \\ P_i^j - G_i + \varepsilon_i\left(\hat{A}_{g_{ii}}^j G_i + \hat{B}_{g_i}Y_i\right)^T & -\varepsilon_i\left(G_i + G_i^T\right) \end{bmatrix} < 0 \\ & P_i^j = {P_i^j}^T > 0, \quad \eta > 0 \\ & i = 1,\dots,N; \quad j = 1,2 \end{aligned} \tag{30}$$

Set $K_i = Y_i G_i^{-1}$.

Step 4: Design pre-filters for controller performance improvement according to (22).

Step 5: Improve the local controllers to minimize the effect of disturbance (load changes) on the voltages at PCCs according to (23).

V. Simulation Results

To verify the performance of the proposed control approach, we consider an islanded inverter-intefaced microgrid consisting of 11 DGs with meshed topology, borrowed from [34], as graphically shown in Fig. 4. The simulation case studies are carried out in MATLAB/SimPowerSystems Toolbox. It is assumed that each DG supports a local load, i.e., a load which is physically connected to the bus terminal of that DG. The

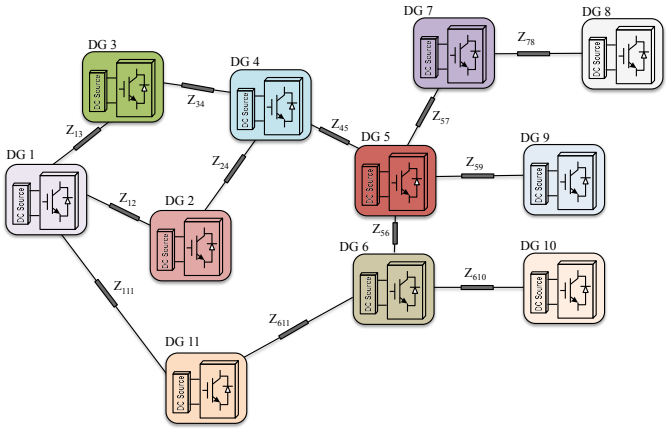

Fig. 4. Layout of an islanded microgrid system composed of 11 DGs.

parameters of all DGs and the transmission lines are given in Table I and Table II, respectively.

TABLE I
ELECTRICAL PARAMETERS OF MICROGRID IN FIG. 4.

DGs	Filter parameters $R_f(m\Omega)$	Filter parameters $L_f(\mu H)$	Shunt capacitance $C_f(\mu F)$	Load parameters $R(\Omega)$	Load parameters $L(\mu H)$	Reference voltages $V_{d_{ref}}$ (pu)	Reference voltages $V_{q_{ref}}$ (pu)
DG 1	1.2	93.7	62.86	76	111.9	0.9	0.436
DG 2	1.6	94.8	62.86	85	134.3	0.9	-0.436
DG 3	1.5	107.7	62.86	93	123.1	0.8	0.6
DG 4	1.5	90.6	62.86	80	167.9	0.8	-0.6
DG 5	1.7	99.8	62.86	125	223.8	0.995	0.1
DG 6	1.6	93.4	62.86	90	156.7	0.6	0.8
DG 7	1.6	109.6	62.86	103	145.5	0.707	0.707
DG 8	1.7	104.3	62.86	150	179	0.9	0.436
DG 9	1.7	100	62.86	81	190.2	0.9	-0.436
DG 10	1.5	99.4	62.86	76	111.9	0.8	0.6
DG 11	1.5	100	62.86	76	111.9	0.6	0.8
DC bus voltage			$V_{dc} = 2000V$				
Power base value			$S_{base} = 8KVA$				
Voltage base value			$V_{base,low} = 0.5KV, V_{base,high} = 11.5KV$				
VSC terminal voltage (line-line)			$V_{VSC} = 600V$				
VSC rated power			$S_{VSC} = 3MVA$				
Transformer voltage ratio			$k_t = 0.6/13.8KV(\Delta/Y)$				
System nominal frequency			$f_0 = 60Hz$				

TABLE II
PARAMETERS OF THE TRANSMISSION LINES IN FIG. 4

Line impedance Z_{ij}	$R_{ij}(\Omega)$	$L_{ij}(mH)$
Z_{12}	1.1	600
Z_{13}	0.9	400
Z_{34}	1	500
Z_{24}	1.2	700
Z_{45}	1	550
Z_{57}	0.7	350
Z_{56}	1.3	800
Z_{59}	1.2	650
Z_{78}	1	450
Z_{610}	1.1	600
Z_{111}	1	700
Z_{611}	1.1	600

Following Algorithm I in Subsection IV-B, all possible connections of DGs to each DG are considered. For example, DG 1 has connections with DG 2, DG 3, and DG 11 ($N_{1_{max}} = \{2,3,11\}$). Moreover, for DG1, the second vertex $A^2_{g_{11}}$ is constructed through the connection with DG 11. Then, local voltage controllers are designed through the convex optimization problem given in (30) which is solved using YALMIP [41] as the interface and MOSEK[2] as the solver.

The dynamic performance of the microgrid system in Fig. 4 with the designed controllers is validated by a set of comprehensive test cases including voltage setpoint variations, PnP operation of DGs, and major changes in the microgrid topology.

[2]Available online in http://www.mosek.com

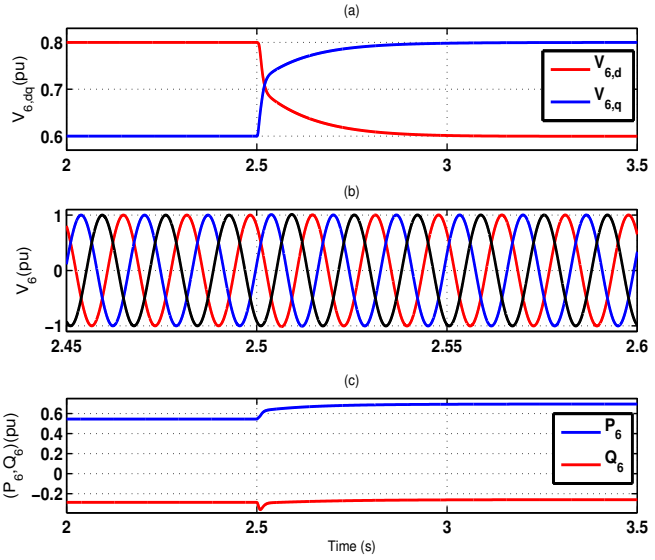

Fig. 5. Dynamic responses of DG 6 due to new reference voltages (a) dq-components of the load voltage at PCC 6, (b) instantaneous load voltages of PCC 6, and (c) output active and reactive power of DG 6.

Case 1: Voltage Tracking Performance Assessment. Consider the microgrid system in Fig. 4 which contains 11 DGs. Each DG provides the active and reactive power for own local loads according to the information/setpoints received from Power Management System (PMS). The dq components of the reference voltages for DGs are initially set according to the values listed in Table I. The d and q components of the reference voltage for DG 6 respectively change from 0.6 pu and 0.8 pu to 0.8 pu and 0.6 pu at $t = 2.5s$. The dynamic responses of DG 6 due to new reference voltages are plotted in Fig. 5. Fig. 5 (a) shows the d and q components of the load voltage of DG 6 and demonstrates that the proposed control strategy successfully regulates the load voltage in less than $0.5s$ with zero steady state error. Fig. 5 (b) and (c) respectively show the instantaneous load voltages of PCC 6 and output active and reactive power of DG 6. Fig. 6 also shows the dq voltages of the other DGs connected to DG 6. The results indicate that there is a short transient (about one cycle of 60 Hz) in the load voltages at PCCs 5, 10, and 11 due to the step change in the setpoints of DG 6.

Case 2: Plug-and-Play Capability. The objective of this case study is to demonstrate the capability of the proposed control strategy in PnP operation of DGs. To conduct this case study, we assume that DG 11 is plugged out at $t = 1.5s$ and due to this failure all the connections attached to DG 11 are disconnected. Therefore, because of this disconnection, dynamics of DG 1 and DG 6 are affected. Then, DG 11 is plugged back into the system at $t = 2.5s$. Dynamic responses of DG 11 and its neighbors due to the PnP functionality of DG 11 are depicted in Fig. 7 and Fig. 8. The results illustrate the robust performance of the proposed control technique

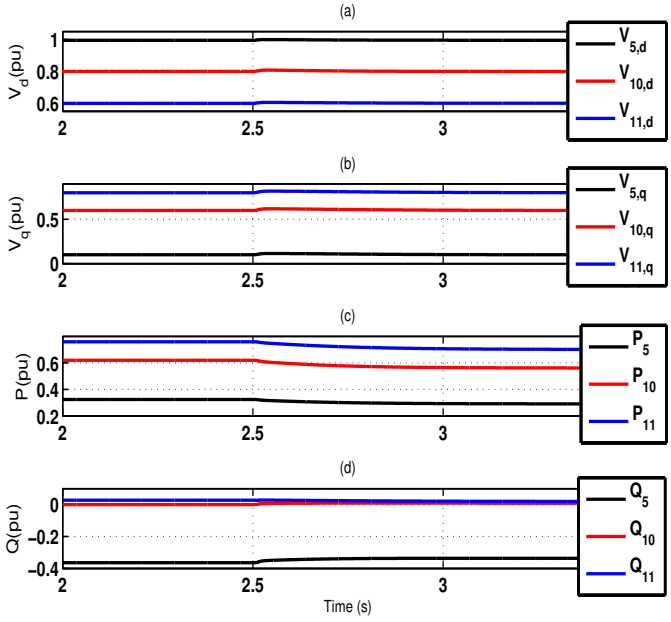

Fig. 6. Dynamic responses of DGs 5,10,11 due to step changes in $V_{dq_{ref_6}}$ (a) d-component of the load voltages at PCCs, (b) q-component of the load voltages at PCCs, (c) output active power of DGs, and (d) output reactive power of DGs.

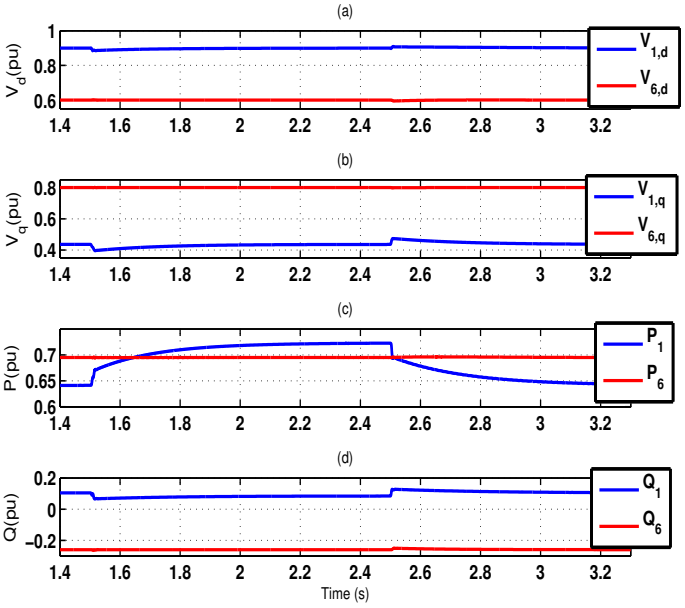

Fig. 8. Dynamic responses of DG 1 and DG 6 due to PnP functionality of DG 11 (a) d-component of the load voltages at PCCs, (b) q-component of the load voltages at PCCs, (c) output active power of DGs, and (d) output reactive power of DGs.

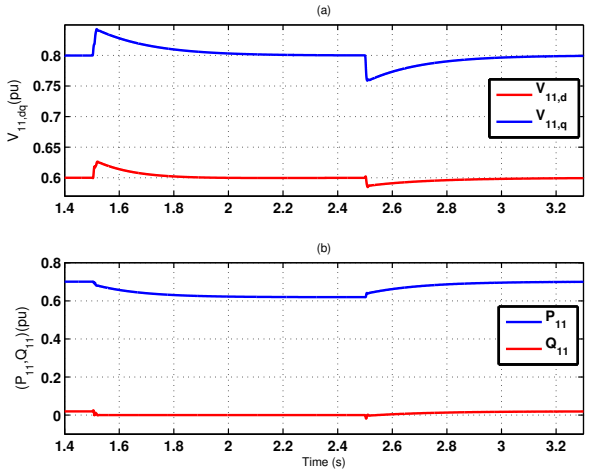

Fig. 7. Dynamic responses of DG 11 when it plugged-out and plugged-in back from/to the microgrid at $t = 1.5s$ and $t = 2.5s$ (a) dq-component of the load voltages at PCC 11 and (b) output active and reactive power of DG 11.

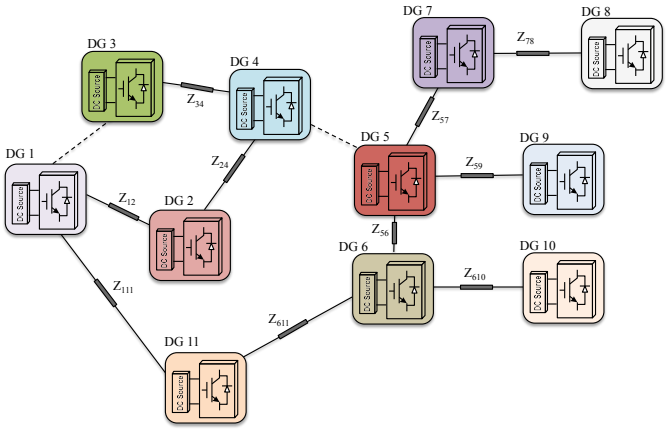

Fig. 9. Layout of the microgrid with a new topology.

to PnP functionality of DGs. The results verify that the voltage controllers guarantee stability and provide a desirable performance according to IEEE standards [42] even in the case of PnP functionality of DGs. Moreover, as the results in Fig. 8 show, the controllers of the neighbours regulate the load voltages at PCCs before, during, and after the PnP operation of DG 11 with a minimum amount of transients.

Case 3: Microgrid Topology Change. The objective of this case study is to assess the robust performance of the local voltage controllers to major topological uncertainties. The topology of the microgrid in Fig. 4 is changed to the configuration of Fig. 9 at $t = 1.5s$. The microgrid transients due to this topology change are illustrated in Fig. 10. The change in the microgrid configuration affects the system dynamics. However, simulation results reveal that the local voltage controllers are able to maintain the stability of the microgrid after a significant change in its configuration.

Case 4: Load Change. In this scenario, the robustness of the controller against the load parameters variations is verified. The load at PCCs is modeled by a three-phase parallel RLC network whose parameters are given in Table I. The dq components of the reference signals of DGs are regulated according to the values listed in Table I. The load resistances

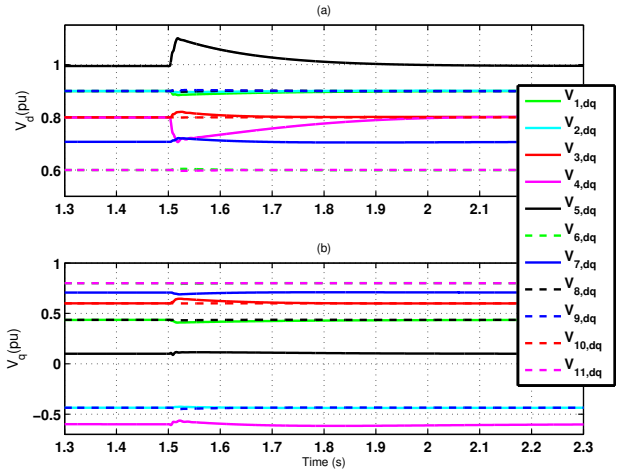

Fig. 10. Dynamic responses of DGs due to a change in microgrid topology at $t = 1.5s$ (a) d-component of the load voltages at PCCs and (b) q-component of the load voltages at PCCs.

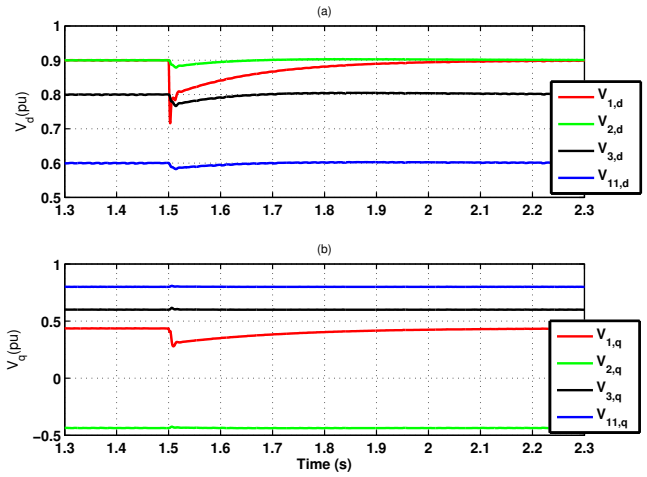

Fig. 11. Voltage signals of DG1 and its neighbors due to a load change at $t = 1.5s$ (a) d-component of the load voltages at PCCs and (b) q-component of the load voltages at PCCs.

R at PCC1 in the three phases are equally changed from 152Ω to 76Ω at $t = 1.5s$. The results which are depicted in Fig. 11 show the robustness of the controller with respect to the load changes.

Case 5: Robustness to Small Deviation in Shunt Capacitors. This case study evaluates the performance of designed control system with respect to small deviation in the shunt capacitors from C_s. To this end, it is assumed that the shunt capacitances in PCC1 and PCC2 are respectively deviated from the common value C_s to $0.9C_s$ and $1.1C_s$. First, the reference voltages for DGs are set according to the values given in Table I. Then, the d and q components of the reference voltage of DG 6 respectively change from 0.6 pu and 0.8 pu to 0.8 pu and 0.6 pu at $t = 2.5s$. The d and q components of all DGs are shown in Fig. 12.

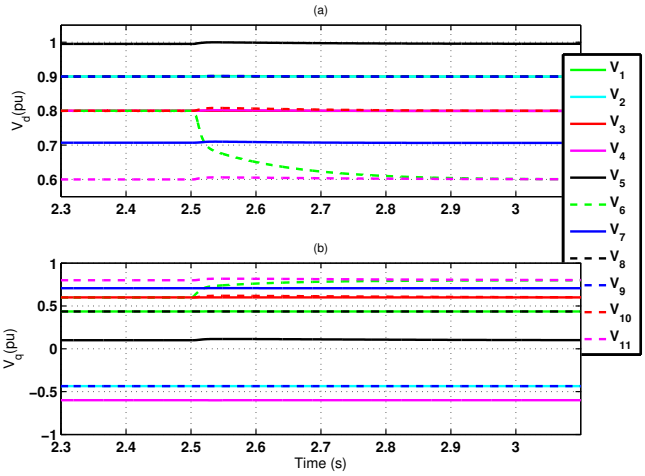

Fig. 12. Voltage signals of DGs due to step changes in $V_{dq_{ref_6}}$ at $t = 2.5s$ and small deviation in C_{t_1} and C_{t_2} (a) d-component of the load voltages at PCCs and (b) q-component of the load voltages at PCCs.

VI. Conclusion

In this paper, a voltage control technique is developed for the islanded operation of inverter-interfaced microgrids with general topology. The control structure is fully decentralized and it relies on the Quasi-Stationary Line (QSL) approximated model of microgrids. The designed controller is the optimal solution of a convex optimization problem using Linear Matrix Inequalities (LMIs). The main features of the proposed control strategy is that local controllers are robust to plug-and-play operation of DGs and microgrid topology change. As a result, the stability of the microgrid system is preserved in the case of plug-in/-out of DGs. The performance of the proposed controller is verified under several case studies, carried out in MATLAB/SimPowerSystems Toolbox, such as voltage tracking, microgrid topology change, plug-and-play capability of DGs, and load changes.

VII. Acknowledgment

The authors acknowledge the CTI - Commission for Technology and Innovation (CH), and the SCCER-FURIES - Swiss Competence Center for Energy Research - Future Swiss Electrical Infrastructure, for their financial and technical support to the research activity presented in this paper.

References

[1] D. E. Olivares, A. Mehrizi-Sani, A. H. Etemadi, C. A. Canizares, R. Iravani, M. Kazerani, A. H. Hajimiragha, O. Gomis-Bellmunt, M. Saeedifard, R. Palma-Behnke, G. A. Jimenez-Estevez, and N. D. Hatziargyriou, "Trends in microgrid control," *IEEE Trans. Smart Grid*, vol. 5, no. 4, pp. 1905–1919, Jul. 2014.

[2] J. M. Guerrero, M. Chandorkar, T. Lee, and P. C. Loh, "Advanced control architectures for intelligent microgrids–Part I: Decentralized and hierarchical control," *IEEE Trans. Ind. Electron.*, vol. 60, no. 4, pp. 1254–1262, Apr. 2013.

[3] A. Parisio, E. Rikos, and L. Glielmo, "A model predictive control approach to microgrid operation optimization," *IEEE Trans. Control Syst. Technol.*, vol. 22, no. 5, pp. 1813–1827, Sep. 2014.

[4] M. Yazdanian and A. Mehrizi-Sani, "Distributed control techniques in microgrids," *IEEE Trans. Smart Grid*, vol. 5, no. 6, pp. 2901–2909, Nov. 2014.

[5] A. Bidram, F. L. Lewis, and A. Davoudi, "Distributed control systems for small-scale power networks: using multi agent cooperative control theory," *IEEE Control Syst. Mag.*, vol. 34, no. 6, pp. 56–77, Dec. 2014.

[6] G. Shafiee, J. M. Guerrero, and J. C. Vasquez, "Distributed secondary control for islanded microgrids–A novel approach," *IEEE Trans. Power Electron.*, vol. 29, no. 2, pp. 1018–1031, Feb. 2014.

[7] J. Schiffer, R. Ortega, A. Astolfi, J. Raisch, and T. Sezi, "Conditions for stability of droop-controlled inverter-based microgrids," *Automatica*, vol. 50, no. 10, pp. 2457–2469, Oct. 2014.

[8] P. Piagi and R. H. Lasseter, "Autonomous control of microgrids," in *Proc. IEEE PES general meeting*, 2006, pp. 1–8.

[9] J. Lopes, C. Moreira, and A. Madureira, "Defining control strategies for microgrids islanded operation," *IEEE Trans. Power Syst.*, vol. 21, no. 2, pp. 916–924, May 2006.

[10] J. C. Vasquez, J. M. Guerrero, A. Luna, P. Rodriguez, and R. Teodorescu, "Adaptive droop control applied to voltage-source inverters operating in grid-connected and islanded modes," *IEEE Trans. Ind. Electron.*, vol. 56, no. 10, pp. 4088–4096, Oct. 2009.

[11] J. C. Vasquez, R. A. Mastromauro, J. M. Guerrero, and M. Liserre, "Voltage support provided by a droop-controlled multifunctional inverter," *IEEE Trans. Ind. Electron.*, vol. 56, no. 11, pp. 4510–4519, Nov. 2009.

[12] R. Majumder, G. Ledwich, A. Ghosh, S. Chakrabarti, and F. Zare, "Droop control of converter-interfaced microsource in rural distributed generation," *IEEE Trans. Power Del.*, vol. 25, no. 4, pp. 2768–2778, Oct. 2010.

[13] J. M. Guerrero, J. C. Vasquez, J. Matas, L. G. de Vicuna, and M. Castilla, "Hierarchical control of droop-controlled AC and DC microgrids–A general approach towards standardization," *IEEE Trans. Ind. Electron.*, vol. 58, no. 1, pp. 158–172, Jan. 2011.

[14] J. Guerrero, P. C. Loh, T. Lee, and M. Chandorkar, "Advanced control architectures for intelligent microgrids–Part II: Power quality, energy storage, and AC/DC microgrids," *IEEE Trans. Ind. Electron.*, vol. 60, no. 4, pp. 1263–1275, Apr. 2013.

[15] J. M. Guerrero, J. C. Vasquez, J. Matas, M. Castilla, and I. G. de Vicuna, "Control strategy for flexible microgrid based on parallel line-interactive UPS systems," *IEEE Trans. Ind. Electron.*, vol. 56, no. 3, pp. 726–736, Mar. 2009.

[16] C.-T. Lee, C.-C. Chu, and P.-T. Cheng, "A new droop control method for the autonomous operation of distributed energy resource interface converters," *IEEE Trans. Power Electron.*, vol. 28, no. 4, pp. 1980–1993, Apr. 2013.

[17] M. Savaghebi, A. Jalilian, J. C. Vasquez, and J. M. Guerrero, "Autonomous voltage unbalance compensation in an islanded droop-controlled microgrid," *IEEE Trans. Ind. Electron.*, vol. 60, no. 4, pp. 1390–1402, Apr. 2013.

[18] P. Kundur, N. J. Balu, and M. G. Lauby, *Power System Stability and Control*. McGraw-Hill Professional, 1994.

[19] M. C. Chandorkar, D. M. Divan, and R. Adapa, "Control of parallel connected inverters in standalone AC supply systems," *IEEE Trans. Ind. Appl.*, vol. 29, no. 1, pp. 136–143, Jan./Feb.1993.

[20] A. H. Etemadi, E. J. Davison, and R. Iravani, "A generalized decentralized robust control of islanded microgrids," *IEEE Trans. Power Syst.*, vol. 29, no. 6, pp. 3102–3113, Nov. 2014.

[21] W. Yao, M. Chen, J. Matas, J. M. Guerrero, and Z.-M. Qian, "Design and analysis of the droop control method for parallel inverters considering the impact of the complex impedance on the power sharing," *IEEE Trans. Ind. Electron.*, vol. 58, no. 2, pp. 576–588, Feb. 2011.

[22] H. Karimi, H. Nikkhajoei, and R. Iravani, "Control of an electronically-coupled distributed resource unit subsequent to an islanding event," *IEEE Trans. Power Del.*, vol. 23, no. 1, pp. 493–501, Jan. 2008.

[23] H. Karimi, E. J. Davison, and R. Iravani, "Multivariable servomechanism controller for autonomous operation of a distributed generation unit: Design and performance evaluation," *IEEE Trans. Power Syst.*, vol. 25, no. 2, pp. 853–865, May 2010.

[24] R. Moradi, H. Karimi, and M. Karimi-Ghartemani, "Robust decentralized control for islanded operation of two radially connected DG systems," in *Proc. IEEE Int. Symp. Ind. Electron. (ISIE)*, Bari, Italy, 2010, pp. 2272–2277.

[25] H. Karimi, A. Yazdani, and R. Iravani, "Robust control of an autonomous four-wire electronically-coupled distributed generation unit," *IEEE Trans. Power Del.*, vol. 26, no. 1, pp. 455–466, Jan. 2011.

[26] A. H. Etemadi, E. J. Davison, and R. Iravani, "A decentralized robust control strategy for multi-DER microgrid-Part I: Fundamental concepts," *IEEE Trans. Power Del.*, vol. 27, no. 4, pp. 1843–1853, Oct. 2012.

[27] B. Bahrani, M. Saeedifard, A. Karimi, and A. Rufer, "A multivariable design methodology for voltage control of a single-DG-unit microgrid," *IEEE Trans. Ind. Informat.*, vol. 9, no. 2, pp. 589–599, May 2013.

[28] M. Babazadeh and H. Karimi, "A robust two-degree-of-freedom control strategy for an islanded microgrid," *IEEE Trans. Power Del.*, vol. 28, no. 3, pp. 1339–1347, Jul. 2013.

[29] S. Riverso, F. Sarzo, and G. Ferrari-Trecate, "Plug-and-play voltage and frequency control of islanded microgrids with meshed topology," *IEEE Trans. Smart Grid*, vol. 6, no. 3, pp. 1176–1184, May 2015.

[30] M. S. Sadabadi, A. Karimi, and H. Karimi, "Fixed-order decentralized/distributed control of islanded inverter-interfaced microgrids," *Control Engineering Practice*, vol. 45, pp. 174–193, Dec. 2015.

[31] M. Cucuzzella, G. P. Incremona, and A. Ferrara, "Design of robust higher order sliding mode control for microgrids," *IEEE Trans. Emerg. Sel. Topics Circuits Syst.*, vol. 5, no. 3, pp. 393–401, Sep. 2015.

[32] ——, "Master-slave second order sliding mode control for microgrids," in *American Control Conference (ACC)*, Chicago, IL, USA, 2015, pp. 5188–5193.

[33] ——, "Third order sliding mode voltage control in microgrids," in *European Control Conference (ECC)*, Linz, Austria, 2015, pp. 2384–2389.

[34] S. Riverso, F. Sarzo, and G. Ferrari-Trecate, "Voltage and frequency control of islanded microgrids: A plug-and-play approach," in *Proc. IEEE Int. Conf. Smart Grid Com.*, Venice, Italy, Nov. 2014, pp. 73–78.

[35] R. Palma-Behnke, C. Benavides, F. Lanas, B. Severino, L. Reyes, J. Llanos, and D. Saez, "A microgrid energy management system based on the rolling horizon strategy," *IEEE Trans. Smart Grid*, vol. 4, no. 2, pp. 996–1006, June 2013.

[36] V. Venkatasubramanian, H. Schattler, and J. Zaborszky, "Fast time-varying phasor analysis in the balanced three-phase large electric power system," *IEEE Trans. Automat. Control*, vol. 40, no. 11, pp. 1975–1982, Nov. 1995.

[37] J. Lunze, *Feedback Control of Large Scale Systems*. NJ, USA: Prentice Hall, 1992.

[38] F. Katiraei and M. R. Iravani, "Power management strategies for a microgrid with multiple distributed generation units," *IEEE Trans. Power Syst.*, vol. 21, no. 4, pp. 1821–1831, Nov. 2006.

[39] F. Katiraei, M. R. Iravani, N. Hatziargyriou, and A. Dimeas, "Microgrids management," *IEEE Power Energy Mag.*, vol. 6, no. 3, pp. 54–65, May-June 2008.

[40] R. C. L. F. Oliveira, M. C. de Oliveira, and P. L. D. Peres, "Robust state feedback LMI methods for continuous-time linear systems: Discussions, extensions and numerical comparisons," in *Proc. IEEE Int. Symp. Comp. Cont. Syst. Design (CACSD)*, Denver, CO, USA, 2011, pp. 1038–1043.

[41] J. Löfberg, "YALMIP: A toolbox for modeling and optimization in MATLAB," in *Proc. IEEE Int. Symp. Comp. Cont. Syst. Design (CACSD)*, 2004. [Online]. Available: http://control.ee.ethz.ch/~joloef/yalmip.php

[42] "IEEE recommended practice for monitoring electric power quality, IEEE standard 1159," 2009.

Mahdieh S. Sadabadi received her Ph.D. in Systems and Control Theory in February 2016 from Electrical Engineering Department, Swiss Federal Institute of Technology in Lausanne (EPFL), Switzerland. Prior to that, she was at the Amirkabir University of Technology (Tehran Polytechnic), Tehran, Iran, where she took a BSc and MSc with honors in Electrical Engineering. She is currently a postdoctoral fellow at the Division of Automatic Control, Department of Electrical Engineering, Linköping University, Linköping, Sweden. Her research interests are centered around fixed-structure controller design, robust control, LMIs, and distributed/decentralized control with applications to energy systems and microgrids.

Qobad Shafiee (S13-M15) received the M.S. degree in Electrical Engineering from the Iran University of Science and Technology, Tehran, Iran, in 2007, and the PhD degree in Electrical Engineering, Microgrids, from the Department of Energy Technology, Aalborg University, Aalborg, Denmark, in 2014. He worked with Department of Electrical and Computer Engineering, University of Kurdistan, Sanandaj, Iran, from 2007 to 2011, where he taught several electrical engineering courses and conducted research on load frequency control of power systems. From March 2014 to June 2014, he was a visiting researcher at the Electrical Engineering Department, University of Texas-Arlington, Arlington, TX, USA. He was a postdoctoral fellow at the Department of Energy Technology, Aalborg University, in 2015. Currently, he is an Assistant Professor at the Department of Electrical & Computer Engineering, University of Kurdistan, Sanandaj, Iran. His main research interests include modeling, power management, hierarchical and distributed control applied to distributed generation in Microgrids.

Alireza Karimi received his B. Sc. and M. Sc. degrees in Electrical Engineering in 1987 and 1990 from Amir Kabir University (Tehran Polytechnic). After 3 years of industrial experience he joined Institut National Polytechnique de Grenoble (INPG) in France and received his DEA and Ph. D. degrees both on Automatic Control in 1994 and 1997, respectively. He was Assistant Professor at Electrical Engineering Department of Sharif University of Technology in Teheran from 1998 to 2000. He is currently Senior Scientist at the Automatic Laboratory of Swiss Federal Institute of Technology in Lausanne (EPFL), Switzerland. He was an Associate Editor of European Journal of Control from 2004 to 2013. His research interests include closed-loop identification, data-driven controller tuning approaches and robust control.